JOURNAL OF GEOPHYSICAL RESEARCH, VOL. 103, NO. E9, PAGES 20,011–20,022, AUGUST 30, 1998

# Galileo observes electromagnetically coupled dust in the Jovian magnetosphere

E. Grün,[1] H. Krüger,[1] A. L. Graps,[2,3] D. P. Hamilton,[4] A. Heck,[1] G. Linkert,[1] H. A. Zook,[5] S. Dermott,[6] H. Fechtig,[1] B. A. Gustafson,[6] M. S. Hanner,[7] M. Horányi,[8] J. Kissel,[1] B. A. Lindblad,[9] D. Linkert,[1] I. Mann,[10] J. A. M. McDonnell,[11] G. E. Morfill,[12] C. Polanskey,[7] G. Schwehm,[13] R. Srama [1]

**Abstract.** Measurements of dust coupled to the Jovian magnetosphere have been obtained with the dust detector on board the Galileo spacecraft. We report on data obtained during the first four orbits about Jupiter that had flybys of the Galilean satellites: Ganymede (orbits 1 and 2), Callisto (orbit 3), and Europa (orbit 4). The most prominent features observed are highly time variable dust streams recorded throughout the Jovian system. The impact rate varied by up to 2 orders of magnitude with a 5 and 10 hour periodicity, which shows a correlation with Galileo's position relative to the Jovian magnetic field. Around 20 $R_J$ (Jupiter radius, $R_J = 71,492$ km) in bound a dip in the impact rate has been found consistently. At the same times, reversals by 180° in impact direction occurred. This behavior can be qualitatively explained by strong coupling of nanometer-sized dust to the Jovian magnetic field. At times of satellite flybys, enhanced rates of dust impacts have been observed, which suggests that all Galilean satellites are sources of ejecta particles. Inside about 20 $R_J$ impacts of micrometer-sized particles have been recorded that could be particles on bound orbits about Jupiter.

## 1. Introduction

In 1973 when the Pioneer 10 spacecraft flew by Jupiter, micron-sized dust particles were detected within the Jovian system for the first time [*Humes et al.*, 1974]. Almost 20 years later the Jovian system was recognized as a source of intermittent streams of submicron-sized dust particles when the Ulysses spacecraft flew by the planet [*Grün et al.*, 1993]. Similar streams were later detected within 2 AU from Jupiter during Galileo's approach to the planet [*Grün et al.*, 1996a].

[1]Max-Planck-Institut für Kernphysik Heidelberg, Germany.
[2]Center for Space Science and Astrophysics, Stanford University, Stanford, California.
[3]Now at Max-Planck-Institut für Kernphysik Heidelberg, Germany.
[4]Department of Physics, University of Maryland, College Park.
[5]NASA Johnson Space Center, Houston, Texas.
[6]Department of Astronomy, University of Florida, Gainesville.
[7]Jet Propulsion Laboratory, Pasadena, California.
[8]Laboratory for Atmospheric and Space Physics, University of Colorado, Boulder.
[9]Lund Observatory, Lund, Sweden.
[10]Max-Planck-Institut für Aeronomie, Katlenburg-Lindau, Germany.
[11]Unit for Space Science and Astrophysics, University of Kent, England.
[12]Max-Planck-Institut für Extraterrestrische Physik, Garching, Germany.
[13]European Space Research and Technology Centre, The Netherlands.



Paper number 98JE00228.
0148-0227/98/98JE-00228$09.00

It was immediately recognized that the magnetosphere of Jupiter would eject submicron-sized dust particles if they existed in the magnetosphere [*Horanyi et al.*, 1993a,b; *Hamilton and Burns*, 1993]. At two places, dust in abundance had been discovered by Voyager's cameras before (1) the Jovian ring at 1.8 $R_J$ (Jupiter radius, $R_J = 71,492$ km) and its weak extension out to 3 $R_J$ [*Showalter et al.*, 1995], and (2) Io's volcanic plumes, which reach heights of about 300 km above Io's surface [*Collins*, 1981]. Both phenomena have been suggested as the source of the dust streams.

Electromagnetic interaction of the particles making up the dust streams was evident both in the Ulysses and Galileo data when both spacecraft were outside the Jovian magnetosphere: the arrival direction showed significant correlations with the ambient interplanetary magnetic field [*Grün et al.*, 1993, 1996a]. *Zook et al.*, [1996] demonstrated convincingly that only particles in the 10 nm size range would couple strongly enough to the interplanetary magnetic field to show the effects observed by Ulysses. Similar analysis of the Galileo data comes to the same result (J.C. Liou, private communication, 1997). The corresponding impact speeds were deduced to be in excess of 200 km/s.

During Galileo's initial approach to Jupiter and Io, dust continuously impacted the dust detector system (DDS), but after Io closest approach, impacts of small particles ceased [*Grün et al.*, 1996b]. A few larger particles were recorded within hours of Jupiter closest ap-

proach. Due to technical constraints, data transmission was very limited and, additionally, the sensitivity of DDS was reduced. Both effects resulted in only a small number of recorded impacts that did not allow a detailed analysis of dust in the inner Jovian magnetosphere. Shortly after Jupiter flyby, DDS was deactivated and was only reactivated half a year later before the first Ganymede flyby.

Galileo's first four orbits through the inner Jovian system are shown in Figure 1. The orbits are named after the satellites Galileo flew by closest: Ganymede, G1 and G2, Callisto, C3, and Europa, E4. Jupiter and the orbits of the Galilean satellites are displayed for comparison. The positions of Galileo and the four satellites at the time of closest approach are given by diamonds. In all four plots the direction to Earth is up.

Galileo is a dual-spinning spacecraft, with an antenna that points antiparallel to the spacecraft positive spin axis (PSA). During most of the orbital tour around Jupiter, the antenna points toward Earth. DDS is mounted on the spinning section of the spacecraft and the DDS sensor axis is offset by an angle of 55° from the spin axis (Figure 2). The rotation angle measures the viewing direction of the dust sensor at the time of particle impact. During one spin revolution of the spacecraft, the rotation angle scans through 360°. DDS rotation angles, however, are reported opposite to that of the actual spacecraft rotation direction [see also *Grün et al.*, 1996a]. This is done for the convenience of easily comparing Galileo DDS results to dust detector data taken on the Ulysses spacecraft. The spin axis of Ulysses points toward Earth. Zero degrees of rotation angle is taken in both cases when the dust sensor points as close as possible to ecliptic north. The rotation angle is taken 90° when the dust sensor axis points parallel to the ecliptic plane in the direction of planetary motion. At rotation angles of 90° and 270° (Figure 2) the sensor axis lies nearly in the ecliptic plane (which corresponds roughly to Jupiter's equatorial plane). DDS has a 140° wide field of view. Dust particles that arrive from within 15° of the PSA can be sensed at all rotation angles, while those that arrive at angles from 15 to 125° from the PSA can only be sensed over a limited range of rotation angles.

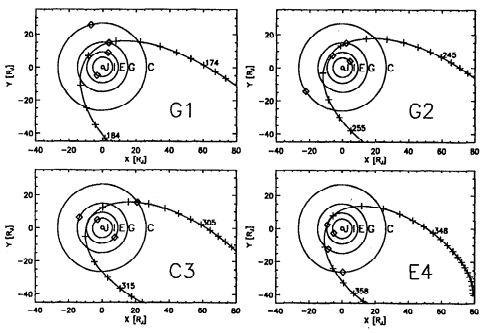


**Figure 1.** Galileo's orbit trajectories during the four satellite flybys projected onto Jupiter's (J) equatorial plane (Jupiter radius, $R_J$ = 71,492 km). The orbits of the Galilean satellites are shown: Io (I), Europa(E), Ganymede (G), and Callisto (C). Dates are marked by crosses (numbers give day of year) on Galileo's paths through the Jovian system. Earth direction is to the top. (top left) Ganymede 1 (June 27, 1996). (top right) Ganymede 2 (September 6, 1996). (bottom left) Callisto 3 (November 4, 1996). (bottom right) Europa 4 (December 19, 1996). All orbits are in counterclockwise direction.

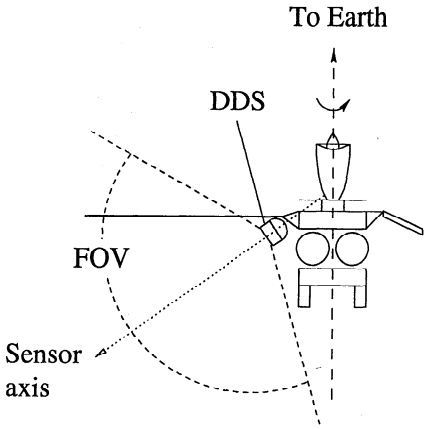


**Figure 2.** Orientation of Galileo: the antenna (top) points toward Earth, and the dust detector system (DDS) largely faces the anti-Earth hemisphere. The sensor axis has an angle of 55° with respect to the positive spin axis (i.e., anti-Earth direction). During one spin rotation of the spacecraft, the sensor axis scans a cone with 110° opening angle. The dust detector itself has 140° field of view. The DDS sensor orientation shown corresponds to a rotation angle of 270° if viewed from the north ecliptic pole.

Now being in a highly elliptical orbit about Jupiter, Galileo performs dust measurements in the inner Jovian magnetosphere and during close flybys of the Galilean satellites. Initial dust measurements have been reported from flybys at Io and Ganymede [*Grün et al.*, 1996b, 1997]. Within the Jovian system at least three different types of dust particles have been identified: (1) small submicron-sized dust particles with high and variable impact rates throughout the Jovian system, (2) a concentration of small dust impacts at the time of Ganymede closest approach, and (3) big micron-sized dust particles concentrated in the inner Jovian system.

In this paper we extend the data set from the two Ganymede flybys already published [*Grün et al.*, 1997] ( hereafter Paper I) and present dust measurements obtained around flybys of Callisto and Europa on November 4 and December 19, 1996. In all time periods considered here, Galileo was within about 100 $R_J$ from Jupiter. Besides the presentation of new data from the four orbits, we concentrate on a discussion of the small dust stream particles.

## 2. Galileo Dust Detector System

The dust detector on board the Galileo spacecraft is a multicoincidence impact ionization detector [*Grün*

*et al.,* 1992a; 1995] which measures submicrometer- and micrometer-sized dust particles. DDS is identical with the dust detector on board Ulysses. For each dust impact onto the detector, three independent measurements of the impact-created plasma cloud are used to derive the impact speed and the mass of the particle. The coincidence times of the three charge signals are used to classify each impact. Class 3, our highest class, are real dust impacts, and class 0 are noise events. Class 1 and class 2 events have been true dust impacts in interplanetary space [*Baguhl et al.,* 1993; *Krüger et al., Three years of Galileo dust data, II, 1993 to 1995, submitted to Planetary Space Science,* 1998]. Within about 15 $R_J$ distance from Jupiter, however, energetic particles cause an enhanced noise rate which affects the class 2 and class 1 events. At the time of this writing, the separation of true dust impacts and noise events in the class 1 and 2 data has not been completed and we consider only class 3 dust impacts throughout this paper.

During most of the time considered here, DDS data were read out either every 7 or every 21 min, depending on the spacecraft data transmission rate, and directly transmitted to Earth (real-time science mode, RTS). For short periods of about an hour around satellite closest approaches (CA), DDS data were collected with a higher rate, recorded on Galileo's tape recorder and transmitted to Earth several days later (record mode). The accuracy with which impact times of individual dust particles can be determined is limited by the readout cycle, i.e., either 7 or 21 min in RTS mode and about 1 min in record mode.

The memory of DDS can store the complete information (counter values, sensor orientation at time of impact, impact charges, signal risetimes, etc.) of up to 40 events. In RTS and record mode the information of

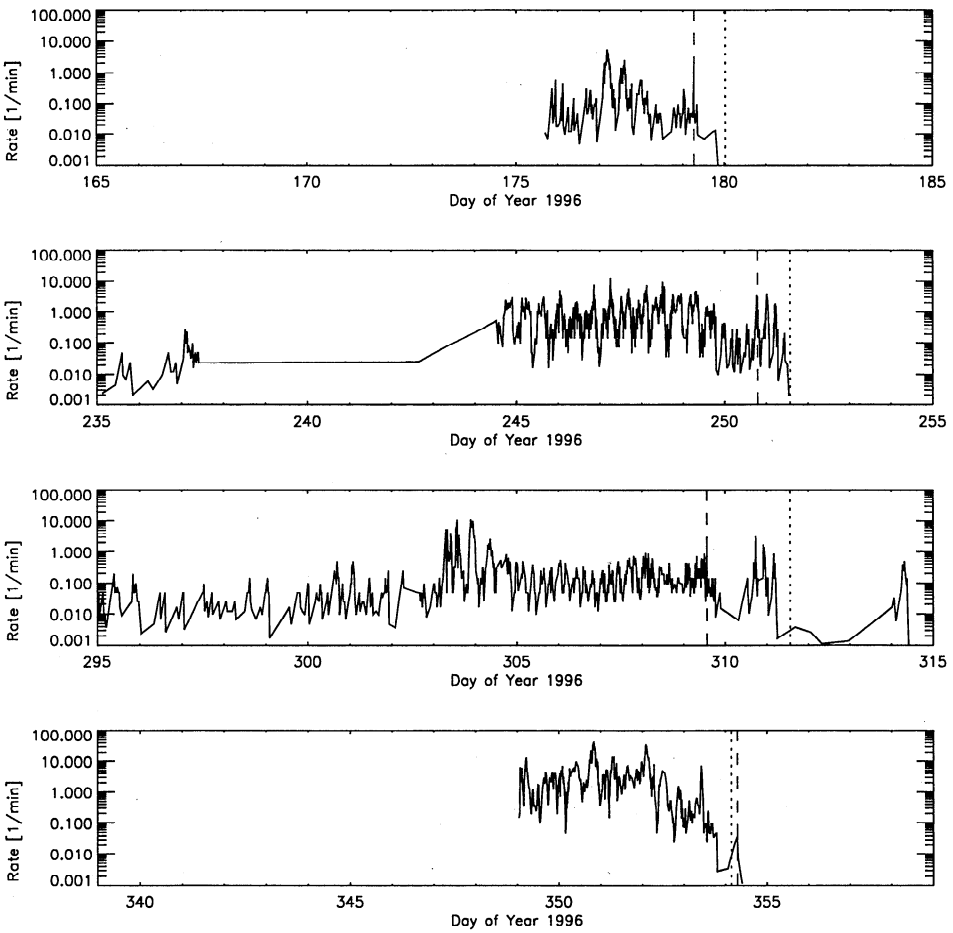


**Figure 3.** Impact rate of small dust particles (impact charge $Q_I < 10^{-13}$ C). The satellite closest approach (dashed line) and perijove passage (dotted line) are indicated. (from top to bottom) (1) Ganymede 1 flyby (June 27, 1996). Shortly after CA (day 179.5 to 181.0), high noise rate caused dead-time which significantly reduced the number of recorded impacts. (2) Ganymede 2 flyby (September 6, 1996). Owing to a spacecraft anomaly, no data were obtained between day 237 and 244. Note the 10 hour periodicity in the impact rate, which is best seen in this panel. (3) Callisto 3 flyby (November 4, 1996). Very few impacts were recorded from day 311 to 313. (4) Europa 4 flyby (December 19, 1996). On day 350 the highest impact rate during the whole orbital tour has been recorded. Note that the dead-time problems which occurred shortly after the Ganymede 1 flyby did not affect the recording of dust impacts during the later satellite flybys due to an optimized instrument configuration.

one impact is read out and transmitted to Earth every readout cycle. Therefore the complete information on each impact is received on the ground when the impact rate is below one impact per either 7 or 21 min in RTS mode or one impact per minute in record mode. When the impact rate is higher, the detailed information of some impacts is lost. In addition, DDS counts all particles with one of 24 accumulators [*Grün et al.*, 1995]. Reliable impact rates could always be calculated from the accumulators, although during times of the highest dust impact rates, the detailed information of a large number of particles could not be transmitted to Earth.

## 3. Results From the Satellite Tour

### 3.1. Dust Particle Impact Rates

In Figure 3 we show the impact rate of our smallest class 3 dust events (ion collector charge $Q_I < 10^{-13}$ C, C = Coulomb) for periods of 20 days around Galileo's G1, G2, C3, and E4 flybys. The dates of CAs were June 27, September 6, November 4, and December 19, 1996. The G1 and E4 data sets cover 8 days around the CAs to Ganymede and Europa (days 175 to 183 and 349 to 357). The G2 data set comprises the period from day 235 to 253 except days 237 to 244, when a spacecraft anomaly (safing) prevented the transmission of data. The C3 data cover the whole period from day 295 to day 315. In Paper I we have presented the dust measurements obtained during a period of 10 days around the first two Ganymede flybys (G1 and G2). Here we recall only the most significant aspects concerning these data.

On days 235 and 295, when Galileo was at a distance of about 100 and 90 $R_J$ from Jupiter, respectively, prior to the G2 and C3 flybys, an impact (imp) rate of about 0.01 imp/min was recorded (Figure 3, but see also Figure 4). DDS was not read out, and hence no data were obtained at that distance during the G1 and E4 orbits. Closer to Jupiter, the impact rate increased by up to 3 orders of magnitude: in all data sets, maxima occurred several days before CA (days 177, 247, 303, and 350). These correspond to distances of 35, 45, 65, and

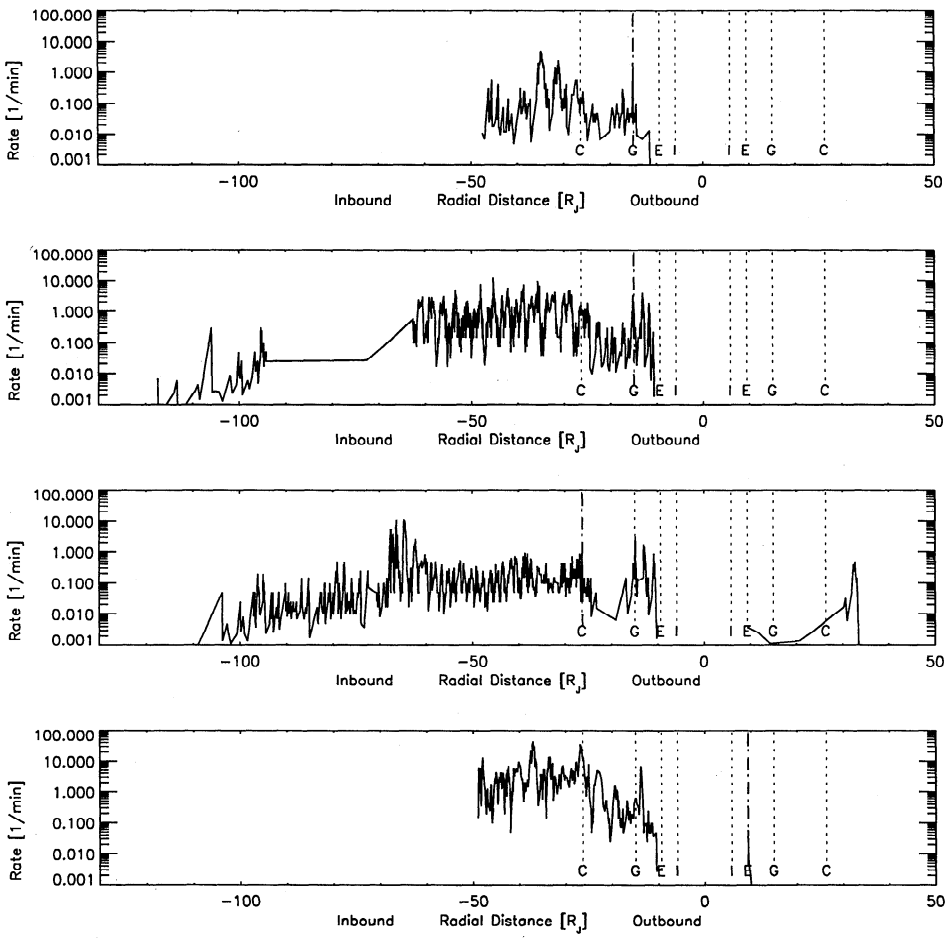


**Figure 4.** Impact rate of small dust particles (impact charge $Q_I < 10^{-13}$ C) versus radial distance from Jupiter. Measurements obtained during inbound (left) and outbound portions are shown separately. The orbits of the Galilean satellites are indicated by dotted lines, and the satellite closest approaches are shown by dash-dotted lines. (from top to bottom) Ganymede 1 flyby (June 27, 1996), Ganymede 2 flyby (September 6, 1996), Callisto 3 flyby (November 4, 1996), Europa 4 flyby (December 19, 1996).

38 $R_J$ from Jupiter, respectively. The impact rates at these maxima were about 10 imp/min in G1, G2, and C3 and 40 imp/min in E4. This last value (day 350) corresponds to the highest impact rate recorded during Galileo's orbital tour so far.

During all four orbits, very few impacts were detected when Galileo was about 20 $R_J$ from Jupiter (days 175.5, 250, 310, and 353). After these local minima, the impact rate increased again for a period of about 1 day (days 179, 251, 310, and 353, where only one spike is seen) when Galileo was about 15 $R_J$ away from Jupiter. Later, close to perijove passage, the detection of small dust impacts nearly ceased (days 180, 251, 311 when very few impacts were still detected, and day 354). In G1 this cessation is partially caused by high noise rates close to perijove passage. This prevented the recording of dust impacts from day 179.5 to 181.0. From day 181 to 183, when the noise rate was low again, no small dust impacts were detected. In all later orbits no such high noise rates occurred in the inner Jovian system because the instrument configuration was changed. For a discussion of the sizes of these particles, see Section 4.

C3 is a special case because a sharp peak of 0.5 imp/min was seen on day 314. Here Galileo was on the outbound part of its orbit at about 33 $R_J$ distance from Jupiter. A few such particles were also detected in the G2 orbit (cf. Section 3.2). At both instances the spacecraft was turned by about 90° away from the nominal Earth pointing direction for a few hours, and dust particles could be sensed that would otherwise be undetectable.

In all four data sets the impact rate shows a fluctuation by up to 2 orders of magnitude with a period of about 10 hours. The 10 hour period most clearly shows up in the G2 data between days 245 and 250. During the G1 and G2 and E4 CAs, sharp spikes occurred, which lasted only about 5 min. A slight increase in the impact rate is also evident at C3 CA.

### 3.2. Impact Directions

The impact direction of the dust particles as derived from the sensor orientation at the time of particle impact is shown in Figure 5. The impact direction of a single particle is only known to lie somewhere within the 140° wide sensitive solid angle cone of DDS. The average of all the rotation angle arrival directions of dust particles belonging to a stream is known to much higher accuracy than is that angle for a single particle.

The impact direction (rotation angle) of dust particles measured along Galileo's trajectory was concentrated between 230° and 310° in the outer Jovian system (days 235 to 237 and 295 to 299, corresponding to a radial distance of 85 $R_J$ to 105 $R_J$ from Jupiter) and widened to a range between 200° and 340° closer to Jupiter. This is compatible with particles approaching from close to the edge of the visible region of DDS far away from Jupiter, whereas closer to Jupiter the impacting stream of particles approached from closer to the center of the DDS field of view when DDS was pointing toward 270° rotation angle.

At a distance of about 20 $R_J$ from Jupiter (days 178.6, 250.2, 310.2, and 353.1) the impact direction shifted by 180°, and dust particles approached from the opposite direction (rotation angles between 20° and 160°). Shortly before the shift, the observed range of rotation angles widened to 360°, and particles seemed to arrive from all directions. This is best seen on day 352 in the E4 data set. Since one half of the DDS viewing angle is 70°, and its viewing direction is offset by only 55° from the positive spin axis, particles approaching from within 15° of the positive spin axis can be detected at all sensor orientations, and hence all rotation angles (cf. Figure 2). On days 254 and 314 (at 33 $R_J$ from Jupiter), a few particles were detected with rotation angles between 200° and 310°, when the spacecraft was turned 90° away from the Earth pointing direction. The particles on day 314 were also seen as a strong peak in impact rate in Figure 3. Particles detected on days 254, 339, and 347 are not considered for the impact rate calculation (Figure 3). Their impact time is known with only 4.2 hour accuracy, which makes the calculation of the impact rate much more uncertain than for the other data.

Particles detected at G1, G2, and E4 CAs came from the direction between 210° and 310°, which is opposite to the approach direction of the stream particles at that time. The vast majority of the particles detected during all four flybys were small submicrometer-sized dust particles that just exceeded the detection threshold (ion collector charge $Q_I \geq 10^{-14}$ C). Twenty-nine bigger ones ($10^{-13}$ C $\leq Q_I \leq 10^{-10}$ C) were detected around and after the satellite CAs. Most of these impacts occurred in the inner Jovian system when Galileo was within 25 $R_J$ from Jupiter, i.e., at a distance comparable to that of the Galilean satellites.

In Figure 6 we show the 2 hour average of the rotation angle of the smallest dust particles ($Q_I < 10^{-13}$ C) from Figure 5. The shift in impact direction from an average value of 270° to 90° around closest approach is clearly visible in all data sets. The 10 hour periodicity first noted in the impact rate (Figure 3) is also evident. Although the impact rate fluctuated on a 10 hour timescale and the range in impact direction widened (Figure 5), the mean impact direction averaged over a few days did not change over a period of several days.

### 3.3. Impact Charge Signals

For each dust impact onto the detector, three independent measurements of the impact-created plasma cloud are used to derive the impact speed and the mass of the particle. The risetimes of the charge signals measured on the target and on the ion collector grid are sensitive to the velocity of the impacting particle [*Grün et al.*, 1995], whereas the amplitudes of the charge signals themselves are sensitive to both mass and speed.

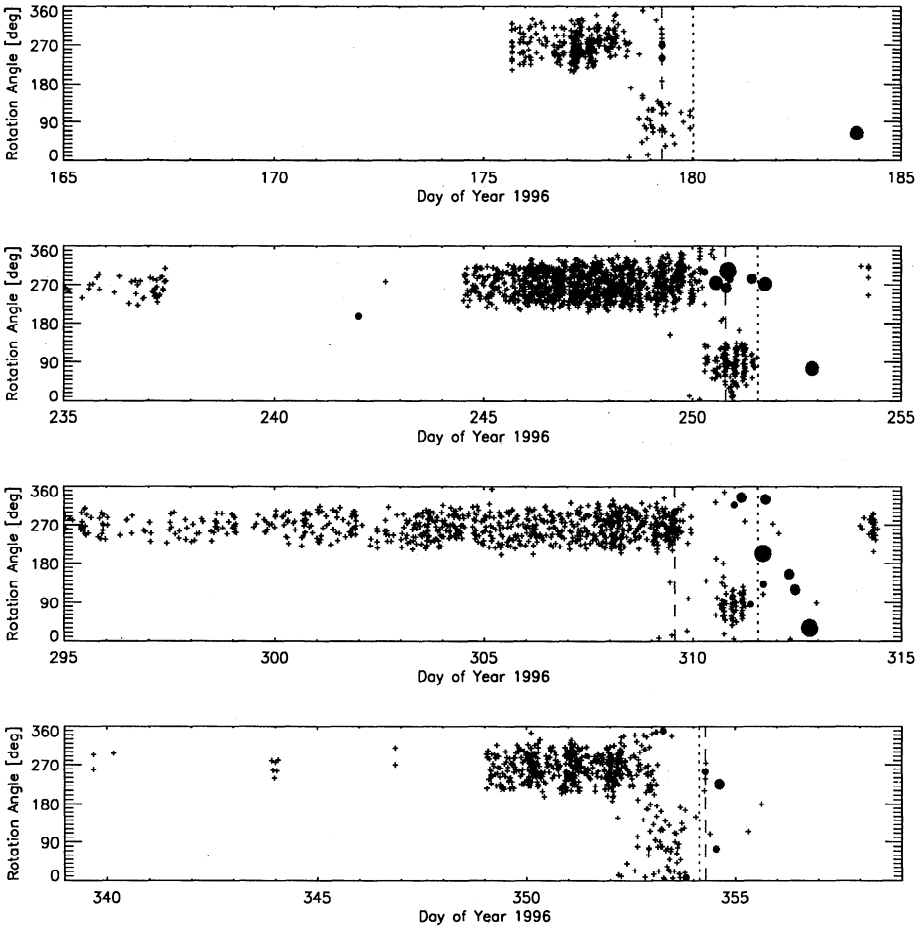


**Figure 5.** Sensor direction at time of dust particle impact (rotation angle) for those impacts for which complete information was available on the ground. Crosses indicate the smallest particles ($Q_I < 10^{-13}$ C). The size of the solid circles indicates the impact charge of the larger particles ($10^{-13}$ C $\leq Q_I \leq 10^{-10}$ C). At 0° the sensor points close to the ecliptic north direction; at 90° and 270° the sensor points close to Jupiter's equatorial plane. The satellite closest approaches are indicated by dashed lines, and the perijove passage by dotted lines. (from top to bottom) Ganymede 1 (June 27, 1996), Ganymede 2 (September 6, 1996), Callisto 3 (November 4, 1996), Europa 4 (December 19, 1996). No data were obtained on days 237 to 244.

Because of the obvious discrepancy between the masses and speeds of stream particles derived via calibration from the measured impact data [*Grün et al.*, 1993] and those values obtained by theoretical analysis [*Zook et al.*, 1996], we refrain from presenting masses and speeds for the observed grains and defer this information to later work. Here we discuss only the raw impact parameters.

The average risetimes of small dust impacts (positive impact charge $\leq 10^{-13}$ C) are shown in Figure 7. Strong fluctuations can be seen; most prominent is the periodic variation during G2 when the 10 hour period is clearly visible. Although it is not so obvious in the G1, C3, and E4 data sets, the 10 hour period is also evident there. Because of the 2 hour averaging of the data, shorter periods (e.g., 5 hours) are depressed. Average amplitudes of the positive impact charge signals ($\leq 10^{-13}$ C) are shown in Figure 8. Also the amplitudes show the 10 hour periodicity. No longer period is obvious. Again the G2 data display the clearest periodicity.

## 4. Discussion

The direction at which a dust impact is sensed depends on the relative speed between Galileo and the dust particle. Therefore, for an analysis of Jovicentric dust trajectories, Galileo's motion has to be taken into account. This is especially true for dust particles orbiting Jupiter at speeds comparable to Galileo's speed (< 20 km/s). For tiny dust particles that travel much faster than Galileo, Galileo's orbit speed displays only a small deviation of their apparent trajectory. For the observation of dust stream particles that are believed to originate in the inner Jovian system, the detection geometry has important consequences. During approach to Jupiter, a radial outflow of dust is initially detected

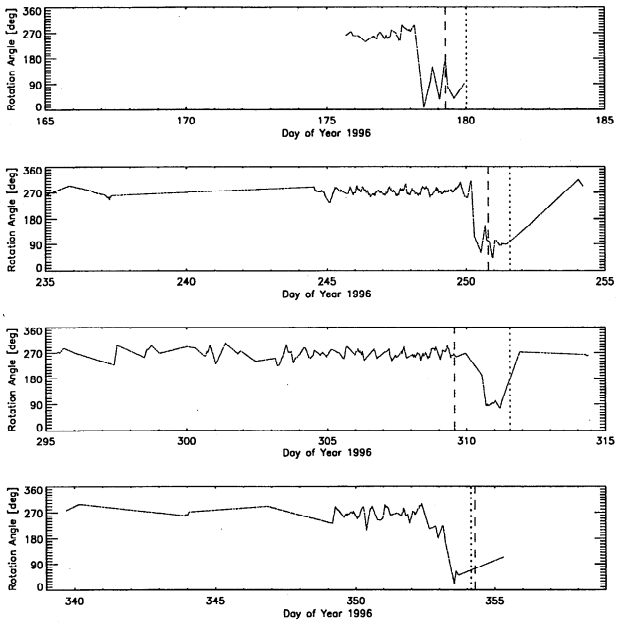


**Figure 6.** Two hour averages of the rotation angle of the small dust particles (impact charge $Q_I < 10^{-13}$ C) shown in Figure 5. The satellite closest approaches are indicated by dashed lines, and perijove passage by dotted lines. (from top to bottom) Ganymede 1 (June 27, 1996), Ganymede 2 (September 6, 1996), Callisto 3 (November 4, 1996), Europa 4 (December 19, 1996).

from rotation angles of 270°. When Galileo moves closer to Jupiter, the impact direction moves closer to the anti-Earth direction, and dust arrives parallel to Galileo's spin axis (if we neglect Galileo's speed). Shortly thereafter, the impact direction changes to rotation angles of 90°. Well past Jupiter CA on Galileo's outbound trajectory, Jupiter and the dust source are in the same hemisphere as the Earth is in when viewed from Galileo. From this direction, dust grains usually cannot enter the DDS sensor, and dust particles remain mostly undetected. This explains why DDS has detected only a few dust particles on the outbound part of the orbits. During the spacecraft turns at 33 $R_J$ in G2 and C3, DDS could detect a few particles there.

Fourier analyses of the observed impact rates have been performed. Figure 9 shows the Fourier transform of the impact rate from day 244.0 to 252.0 during the Ganymede 2 encounter. The most significant peaks in the frequency spectrum are close to 10 hours (Jupiter's spin period) and at about half that period. Because of the short time interval which was analyzed, no lower frequencies are evident. All four sets of encounter data show a similar behavior. The highest peaks are always at Jupiter's rotation frequency and twice that value.

To study the phase relation between Jupiter's magnetic field at the position of Galileo and the various impact parameters, we have a closer look at a subset of the G2 data in Figure 10. The upper panel shows Galileo's distance from the magnetic equatorial plane ($Z$ position in Jupiter's magnetic field; a tilted dipole field has been adopted). The lower panels show 2 hour averages of the observed impact rate, impact direction, risetime $t_I$ and amplitude $Q_I$ of the ion charge signal. The 5 and 10 hour periodicities are evident in all observed impact data. Maxima in impact rate occur when Galileo is at its lowest position in the magnetic field, and minima in impact rate are coincident with Galileo's highest position in the magnetic field. Thus the maxima and minima in impact rate occur when Galileo "sees" a vanishing velocity component of the magnetic field in the $Z$ direction. The rotation angle, $t_I$ and $Q_I$ are also correlated with the magnetic field position. This indicates that the impact direction, impact velocity, and sizes of the impacting dust particles are modulated by the magnetic field. The maxima in impact rate are coincident with minima in the rotation angle and vice versa. Finally, the impact rate is anticorrelated with $t_I$ and correlated with $Q_I$.

In order to demonstrate some characteristics of dust that couples electromagnetically to the magnetosphere we employ a simple model of dust released in the inner Jovian magnetosphere [cf. *Horanyi et al.*, 1993a, b; *Hamilton and Burns*, 1993]. As an example, we use Io as a point source for nanometer-sized dust. The basic assumptions of the model are that dust is released from Io with its Jovicentric orbital speed of $v = 17.4$ km/s. We assume a dust density of $\rho = 1000$ kg/m$^3$ and an instantaneous charging to $U_g = +3$ V surface potential;

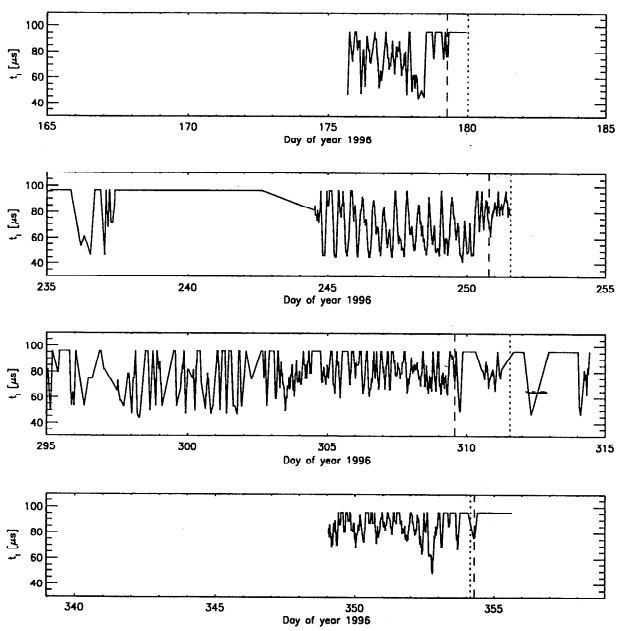


**Figure 7.** Risetime $t_I$ of the charge signal measured on the ion collector grid. The panels show a 2 hour average of the indvidual risetimes measured. The satellite closest approaches are indicated by dashed lines and perijove passage by dotted lines. (from top to bottom) Ganymede 1 (June 27, 1996), Ganymede 2 (September 6, 1996), Callisto 3 (November 4, 1996), Europa 4 (December 19, 1996).

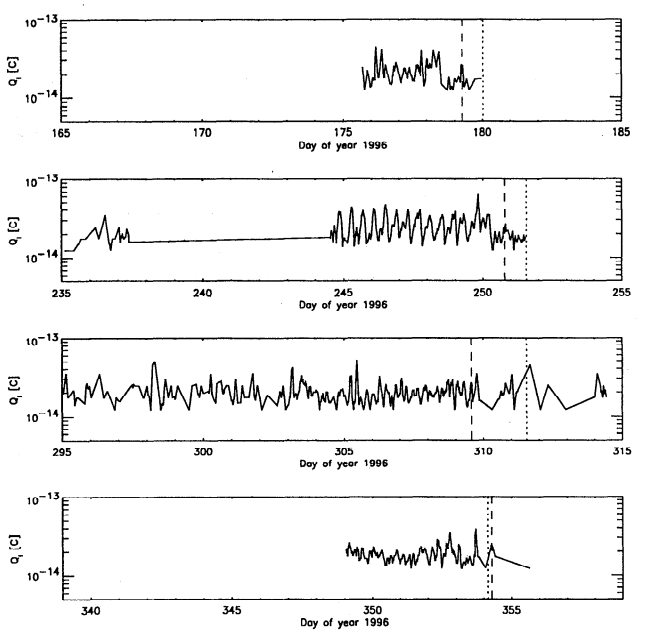


**Figure 8.** Impact-created plasma charge $Q_I$ measured on the ion collector grid. Again, 2 hour averages are shown and the satellite closest approaches are indicated by dashed lines and perijove passage by dotted lines. (from top to bottom) Ganymede 1 (June 27, 1996), Ganymede 2 (September 6, 1996), Callisto 3 (November 4, 1996), Europa 4 (December 19, 1996).

a more realistic charging scenario is given by *Horanyi et al.* [1993b, 1997]. For Jupiter's magnetic field we assume a tilted (9.6°) dipole that rotates rigidly with Jupiter. Beyond a distance of 50 $R_J$, the magnetic field deviates strongly from the assumed configuration, but there the electromagnetic effects are weak and therefore are neglected. Forces that a particle of mass $m$ feels are Jupiter's gravity

$$\vec{F}_G = \frac{GM_J m}{r^3}\vec{r}; \quad (1)$$

with $GM_J = 1.27 \times 10^{17}\mathrm{m^3 s^{-2}}$, particle mass $m = (4\pi/3)\rho s^3$, and the Lorentz force

$$\vec{F}_L = q\left(\vec{v}\times\vec{B}+\vec{E}\right) \quad (2)$$

The charge on a dust particle of radius $s$ is given by $q = 4\pi\epsilon_0 U_g s$, with permittivity $\epsilon_0 = 8.859\times10^{-12}$ C/(V m). For example, a $s = 9$ nm radius particle carries about 20 elementary charges. Electromagnetic forces dominate the motion of small particles ($s \lesssim 30$ nm). For these particles the parameter

$$\frac{q}{m} = \frac{3\epsilon_0 U_g}{\rho s^2} \quad (3)$$

describes their dynamics. The magnetic field magnitude in the magnetic equatorial plane is

$$B = B_0\left(\frac{R_J}{r}\right)^3 \quad (4)$$

with ($B_0 = 4.2\times10^{-4}$T). The corotational electric field $\vec{E}$ points away from Jupiter, and its magnitude is given by

$$E = 5.3\left(\frac{R_J}{r}\right)^2 \mathrm{V/m} \quad (5)$$

and can formally be derived from a potential

$$U_{co} = 3.6\times10^8\,\frac{R_J}{r}\mathrm{V} \quad (6)$$

i.e., at Io's orbit, this potential corresponds to about +60 MV.

It can easily be shown [*Horanyi et al.*, 1993a, b; *Hamilton and Burns*, 1993] that positively charged dust grains in a certain size range are driven out of the magnetosphere by the corotational electric field. Figure 11 shows trajectories of dust particles that are released from Io into the magnetosphere. At Io's distance ($r = 5.9\ R_J$), particles from about 9 nm to 180 nm radius are accelerated outward and leave the Jovian system. Smaller particles remain tied to the magnetic field lines and gyrate around them like ions do. Larger particles move on gravitationally bound orbits that are more or less affected by the Lorentz force. Escaping particles in the middle size range have straight trajectories with local tangents passing Jupiter close to or even inside the source distance. The largest and the smallest escaping particles have more curved trajectories.

The size range of expelled particles narrows down if the source is located closer to Jupiter, with the upper size limit staying about constant at 180 nm. At the outer distance of the gossamer ring (3 $R_J$) the lower size limit is already 28 nm [*Hamilton and Burns*, 1993]. At the corotational distance (2.2 $R_J$ where the Keplerian orbit period equals Jupiter's rotation) the Lorentz force on ring particles vanishes, and no particles can escape. Because of the radial variation of the lower size limit of expelled particles, this size is an indication of the source distance from Jupiter.

Besides the outward acceleration, there is a significant out-of-plane component of the electromagnetically

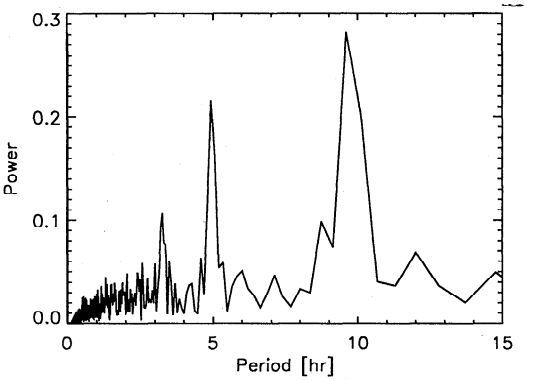


**Figure 9.** Fourier transforms of G2 impact rate data from day 244.0 to 252.0. Jupiter's spin period is 9 hours 55 min 30 s for comparison.

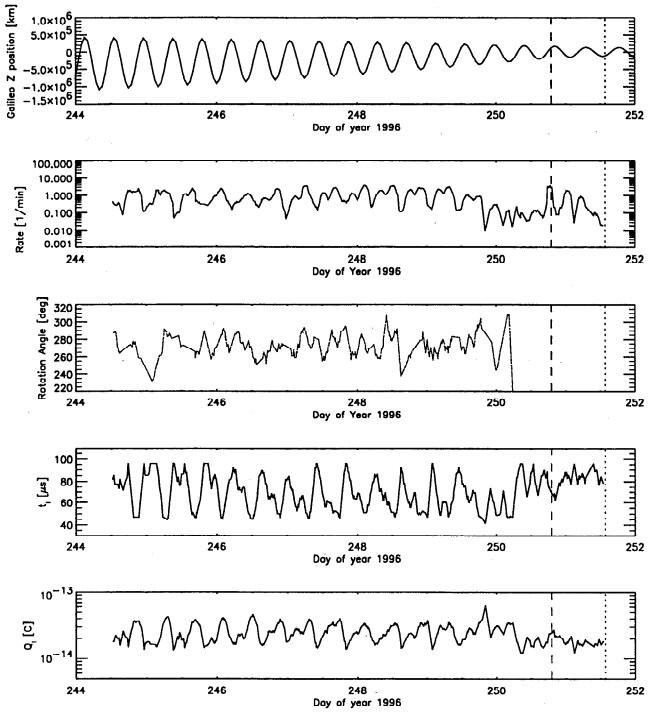


**Figure 10.** A subset of the Ganymede 2 data. Phase relation between Galileo's position in Jupiter's magnetic field (here Galileo's distance from the magnetic equatorial plane is shown) and observed impact rate, impact direction, ion charge risetime $t_I$ and ion charge amplitude $Q_I$. A dipole tilted by 9.6° with respect to Jupiter's rotation axis pointing toward $\lambda_{III} = 202°$ has been adopted for the magnetic field. The observed data are smoothed with a 2 hour average. The closest approach to Ganymede is indicated by dashed lines, and perijove passage by dotted lines.

induced force. Depending on the phase of the inclined magnetic field (with respect to Jupiter's rotation) at the position of the particle, its trajectory is deflected out of Jupiter's equatorial plane where the particle originated.

For those particles that eventually leave the Jovian system the main acceleration occurs within a short distance from the source. In Figure 12 the Jovicentric speeds of particles of different sizes are displayed as a function of distance to Jupiter. For positively charged particles of 120 nm radius that originate at Io's orbit the corotational electric field nearly cancels the gravitational field of Jupiter and keeps the initial kinetic energy. Larger particles for which the gravitational field exceeds the corotational field lose kinetic energy and are decelerated. Particles smaller than about 50 nm radius are strongly accelerated and reach already about 70% of their terminal speed at a distance of 10 $R_J$ from Jupiter and move there on roughly straight trajectories. The escape speed from the Jovian system of the smallest particles that originate from Io's distance is about 350 km/s. Because of the dependence of the lower size limit of escaping particles, the escape speed of the smallest particles originating from 3 $R_J$ is "only" 120 km/s.

Dust particles that are continuously released from a point source escape in a warped sheet of dust, where particles are separated according to their size (or more appropriately their $q/m$ ratio) and time of generation. This scenario is depicted in Figure 13 for two different phases of the Jovian magnetic field showing two snapshots of the dust sheet. The ragged outer edge of the dust sheet is caused by the fact that dust trajectories have been followed only out to 50 $R_J$, in steady state the dust sheet extends to much larger distances. Following a concept of comet tail physics [*Finson and Probstein,* 1968], the solid lines (synchrones) show positions of particles released at the same time $\tau$ before the observation. Synchrones near the source correspond to release times close to the time of observation. The release time difference between adjacent synchrones is 1332 s (the number of time steps is given by bold numbers). The oldest synchrone shown corresponds to a release time 25.9 hours (corresponding to two Jupiter rotations as seen from Io) prior to observation.

Positions of equal-sized particles or, more appropriately, of particles of the same $q/m$ value, are shown by dashed curves. Positions of 30 different $q/m$ values are shown ($q/m$ values are given by italic numbers). We have limited the sizes to $s \leq 100$ nm ($q/m \geq 8$ C/kg); bigger and thus slower particles would still be closer to the source. The configuration of the dust sheet depends strongly on the phase of the magnetic field. Only the $\tau = 0$ position stays at the source, all other $(q/m, \tau)$ positions move around with Jupiter's rotation period of 9.92 hous. The vertical excursions, in particular, show this periodicity. The dust density in the sheet at position $(q/m, \tau)$ is determined by the source strength of particles in both the $q/m$ interval, $[q/m, q/m + \Delta q/m]$,

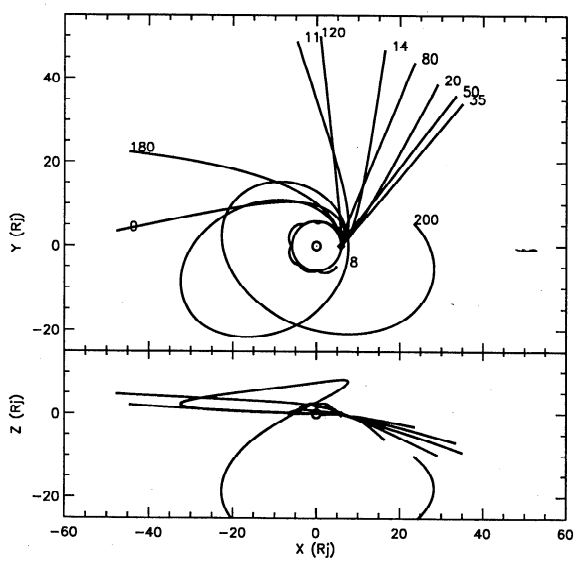


**Figure 11.** Trajectories of dust grains released from an Io source shown in the Jovian equatorial plane ($x - y$) and a perpendicular plane ($x - z$). The numbers give the grain radius in nm. The assumed grain charge corresponds to a surface potential of +3 V.

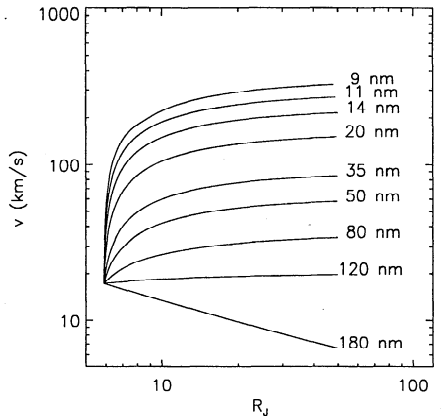


**Figure 12.** Speeds of dust grains escaping from Io's orbit. The numbers indicate the grain sizes (surface potential +3 V).

the release time interval $[\tau, \tau + \Delta\tau]$, and the area of that part of the dust sheet that is bordered by the corresponding synchrones and syndynes. That means the dust sheet is, in general, not uniformly populated by dust.

An observer in Jupiter's equatorial plane would record dust particles when the warped dust sheet passes over its position. This occurs about twice per Jupiter rotation, and a periodic flux results with a 5 hour periodicity. For a moving observer (e.g., Galileo), this period is somewhat altered according to the angular motion of the observer. Since the dust sheet is fixed to the source, it moves around Jupiter with the source's orbital period (e.g., $P_{Io} = 42.4$ hours). Dust particles of different sizes ($q/m$ values) would be recorded at different times during one orbital period.

The dust impact rate observed by Galileo clearly shows 5 and 10 hour periodicity but a longer orbital period, such as Io's, is not very obvious in the data. Therefore it is concluded that the source from which the particles freely escape is rather extended. If the source is azimuthally extended, like the Io torus or a ring, the dust flux can be thought of as a superposition of many dust sheets fixed to different positions of the source region. In this case an observer at any position would see dust particles from dust sheets that pass over its position at all times. However, the sizes and corresponding speeds of dust particles would vary with about 5 and 10 hour periodicity. In this case the fluctuations of the impact rate reflect the size distribution at the source. Those particles that are generated most abundantly would show up most prominently in the impact rate. This scenario seems to describe the observed periodicities most accurately. However, some other features of the data, e.g., the more or less flat impact rate inside 50 $R_J$ during Galileo's approach to Jupiter or the

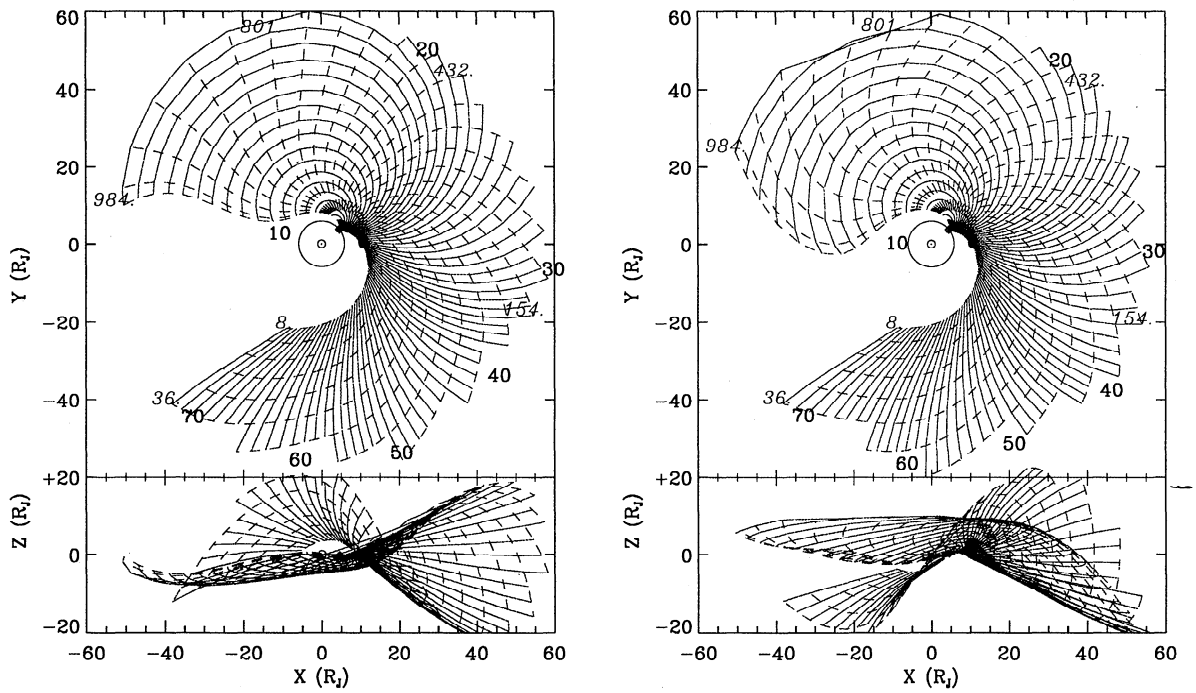


**Figure 13.** Dust sheet at two different phases of the magnetic field (0° and 120°). The dust sheet is defined by synchrones (solid lines, positions of dust particles that were released at the same time) and syndynes (dashed lines, positions of dust particles that have the same charge-to-mass ratio, $q/m$). Adjacent synchrones are 1332 s apart. The number of time steps (synchrones) prior to observation is given by bold numbers (synchrones 0 to 70). The oldest synchrone is about 2.2 days old (synchrone 70). Syndynes of differently sized particles range from $s = 9.0$ nm to $s = 100$ nm, or, alternatively, at a surface potential of $U_g = +3$ V to different $q/m$ values: 984, 979, 962, 935, 898, 853, 801, 744, 682, 619, 555, 492, 432, 374, 320, 271, 227, 188, 154, 125, 100, 79, 62, 48, 36, 27, 21, 15, 11, and 8 C/kg.

dip in impact rate around 20 $R_J$ need additional effects that have been numerically modeled by *Horanyi et al.* [1997].

As noted earlier (Paper I), there is a second category of particles, which occurred within a few minutes of the satellite encounters. It has the signature of dust released from that satellite: the impact rate is strongly peaked at the time of CA, and the impact direction is compatible with a satellite source (note that only particles arriving from about 270° can be explained by a satellite source, whereas 90° is not compatible with such a source). The 270° category is noticeable during all encounters. A preliminary discussion can be found in Paper I, but a detailed analysis is forthcoming.

Large-particle impacts have been recorded during all four passages through the inner Jovian system. Note that during the G1 passage from day 179.5 to 181.0, no impacts could be recorded due to dead-time problems. Large-particle impacts behave quite differently from dust stream particles (cf. Figure 5): their impact rate peaks near perijove, where the change of rotation angle occurs. Such a population of particles has also been observed by previous spacecraft carrying dust detectors through the Jovian system: Pioneers 10 and 11 [*Humes,* 1980] and Ulysses [*Grün et al.,* 1992b]. Large-particle impacts prior to perijove with rotation angles of about 270° are compatible with particles orbiting on prograde or retrograde orbits, whereas postperijove impacts with rotation angles of 90° can best be explained by highly inclined or even retrograde orbits. A discussion of a mechanism that provides micron-sized dust in the inner Jovian magnetosphere on both prograde and retrograde orbits can be found in a companion paper [*Colwell et al.,* this issue].

## 5. Summary and Conclusions

During the first four orbits around Jupiter, the Galileo dust detector recorded a highly variable impact rate that had characteristic and repeating signatures. Here is a summary of the observations and possible explanations.

1. The main signature of the data, namely the 5 and 10 hour periodicities of impact rate, direction, signal amplitude and risetime are most naturally explained by the coupling of charged dust particles to Jupiter's magnetic field. However, the source region has to be extended; a point source would cause a strong additional periodicity with its longer orbital period. A possible extended source is the cold Io plasma torus that has the effect of dispersing negatively charged dust particles all around the torus [*Hamilton,* 1996] before their charge eventually reverses and they are released [*Horanyi et al.,* 1997].

2. Sporadic strong fluctuations of the impact rate on timescales of 1 day are most probably explained by variations in the transport conditions or in the source strength. However, no correlations with other observations, e.g., changes in magnetospheric plasma parameters or plume activity on Io, have yet been found.

3. The more or less flat impact rate inside 50 $R_J$ during Galileo's approach to Jupiter and the dip in impact rate around 20 $R_J$ have been explained by asymmetries in the Io torus and the subsequent preferential dust release from the torus on the duskside of Jupiter [*Horanyi et al.,* 1997].

4. There were vanishing impact rates shortly before Jupiter closest approach and on the outbound trajectory, except for short bursts at about 40 $R_J$ distance. This is a purely geometric effect being caused by the attitude of the spacecraft, the aperture of the dust sensor, and dust trajectory directionality. Dust particles escaping from the inner Jovian system cannot enter the dust sensor near and after Jupiter closest approach. The details of this effect depend on how straight or how strongly curved the trajectories are.

5. The shifts in impact direction by 180° at 20 $R_J$ inbound and at 40 $R_J$ outbound are also a geometric effect because they depend on where Galileo is with respect to the source region and the Jupiter-Earth line. The exact position where the transition from one to the other impact direction occurs depends on how strongly the trajectories are bent. The best match with the data are tiny particles (about 10 nm radius) that have strongly curved trajectories.

6. Enhanced impact rates within minutes of closest approach to the satellites indicate a population of ejecta particles from these satellites.

7. Inside a distance of about 20 $R_J$ from Jupiter, impacts of large particles have been recorded. Their impact direction changes by 180° at about the time of perijove. Some impacts are compatible with particles on prograde orbits, but there has to be a significant fraction of particles on retrograde orbits as well.

These data alone do not definitively identify the ultimate source of the dust stream particles, although the data seem to be compatible with an Io/Io torus source. The strongest argument so far comes from the analysis of *Zook et al.* [1996], who pointed out that the observed coupling to the interplanetary magnetic field can only be explained if the particles have sizes of about 10 nm. Such sizes argue rather for an Io source than for a gossamer ring source. In addition, modeling of an Io source and the complex interaction with the Io torus succeeded in a satisfactory match to the data. More data and more modeling are needed in order to finally answer this question.

**Acknowledgments.** We thank the Galileo project at JPL for effective and successful mission operations. This work has been supported by the Deutsche Agentur für Raumfahrtangelegenheiten (DARA).

## References

Baguhl, M., E. Grün, G. Linkert, D. Linkert, N. Siddique, and H. Zook, Identification of "small" dust impacts in

the Ulysses dust detector data, *Planet. Space Sci.*, 41, 1085-1098, 1993.

Collins, S. A., Spatial color variations in the volcanic plume at Loki, on Io, *J. Geophys. Res.*, *86*, 8621-8628, 1981.

Colwell, J. E., M. Horányi, and E. Grün, Jupiter's exogenic dust ring, *J. Geophys. Res*, this issue.

Finson, M., and R. Probstein, A theory of dust comets, I., Model and equations, *Astrophys. J.*, *154*, 327, 1968.

Grün, E., H. Fechtig, M. S. Hanner, J. Kissel, B.-A. Lindblad, D. Linkert, G. Linkert, G. E. Morfill, and H. Zook, The Galileo dust detector, *Space Sci. Rev.*, *60*, 317-340, 1992a.

Grün, E., H. A. Zook, M. Baguhl, H. Fechtig, M. S. Hanner, J. Kissel, B.-A. Lindblad, D. Linkert, G. Linkert, I. Mann, J. A. M. McDonnell, G. E. Morfill, C. Polanskey, R. Riemann, G. Schwehm, and N. Siddique, Ulysses dust measurements near Jupiter, *Science*, *257*, 1550-1552, 1992b.

Grün, E., H. A. Zook, M. Baguhl, A. Balogh, S. J. Bame, H. Fechtig, R. Forsyth, M. S. Hanner, M. Horányi, J. Kissel, B.-A. Lindblad, D. Linkert, G. Linkert, I. Mann, J. A. M. McDonnell, G. E. Morfill, J. L. Phillips, C. Polanskey, G. Schwehm, N. Siddique, P. Staubach, J. Svestka, and A. Taylor, Discovery of Jovian dust streams and interstellar grains by the Ulysses spacecraft, *Nature*, *362*, 428-430, 1993.

Grün, E., M. Baguhl, D. P. Hamilton, J. Kissel, D. Linkert, G. Linkert, and R. Riemann, Reduction of Galileo and Ulysses dust data, *Planet. Space Sci.*, *43*, 941-951, 1995.

Grün, E., M. Baguhl, D. P. Hamilton, R. Riemann, H. A. Zook, S. Dermott, H. Fechtig, B. A. Gustafson, M. S. Hanner, M. Horányi, K. K. Khurana, J. Kissel, M. Kivelson, B.-A. Lindblad, D. Linkert, G. Linkert, I. Mann, J. A. M. McDonnell, G. E. Morfill, C. Polanskey, G. Schwehm, and R. Srama, Constraints from Galileo observations on the origin of Jovian dust streams, *Nature*, *381*, 395-398, 1996a.

Grün, E., D. P. Hamilton, R. Riemann, S. Dermott, H. Fechtig, B. A. Gustafson, M. S. Hanner, A. Heck, M. Horányi, J. Kissel, H. Krüger, B.-A. Lindblad, D. Linkert, G. Linkert, I. Mann, J. A. M. McDonnell, G. E. Morfill, C. Polanskey, G. Schwehm, R. Srama, and H. A. Zook, Dust measurements during Galileo's approach to Jupiter and Io encounter, *Science*, *274*, 399-401, 1996b.

Grün, E., H. Krüger, S. Dermott, H. Fechtig, A. Graps, B. A. Gustafson, D. P. Hamilton, M. S. Hanner, A. Heck, M. Horányi, J. Kissel, B.-A. Lindblad, D. Linkert, G. Linkert, I. Mann, J. A. M. McDonnell, G. E. Morfill, C. Polanskey, G. Schwehm, R. Srama, and H. A. Zook, Dust measurements in the Jovian magnetosphere, *Geophys. Res. Lett.*, *24*, 2171-2174, 1997.

Hamilton, D. P., Dust from Jupiter's gossamer ring and the Galilean satellites, *Bull. Am. Astron. Soc.*, *28*, 1123, 1996.

Hamilton, D. P., J. A. Burns, Ejection of dust from Jupiter's gossamer ring, *Nature*, *364*, 695-699, 1993.

Horányi, M., G. E. Morfill, and E. Grün, Mechanism for the acceleration and ejection of dust grains from Jupiter's magnetosphere, *Nature*, *363*, 144-146, 1993a.

Horányi, M., G. E. Morfill, and E. Grün, The dusty ballerina skirt of Jupiter, *J. Geophys. Res.*, *98*, 21,245-21,251, 1993b.

Horányi, M., E. Grün, and A. Heck, Modeling the Galileo dust measurements at Jupiter, *Geophys. Res. Lett.*, *24*, 2175-2178, 1997.

Humes, D. H., J. M. Alvarez, R. L. O'Neal, and aW. H. Kinard, The interplanetary and near-Jupiter meteoroid environments, *J. Geophys. Res.*, *79*, 3677, 1974.

Humes, D. H., Results of Pioneer 10 and 11 meteroids experiments: Interplanetary and near-Saturn, *J. Geophys. Res.*, 85, 5841-5852, 1980.

Showalter, M. R., J. A. Burns, J. N. Cuzzi, J. B. Pollack, Discovery of Jupiter's 'gossamer' ring, *Nature*, *316*, 526-528, 1985.

Zook, H. A., E. Grün, M. Baguhl, D. P. Hamilton, G. Linkert, J.-C. Liou, R. Forsyth, and J. L. Phillips, Solar wind magnetic field bending of Jovian dust trajectories, *Science*, *274*, 1501-1503, 1996.

---

S. Dermott and B.A . Gustafson, Department of Astronomy, University of Florida, Gainesville, FL 32611.

H. Fechtig, A. Graps, E. Grün, A. Heck, J. Kissel, H. Krüger, D. Linkert, G. Linkert, and R. Srama, Max-Planck-Institut für Kernphysik, Saupfercheckweg 1, 69117 Heidelberg, Germany.

D.P. Hamilton, Department of Physics, University of Maryland, College Park, MD 20742-2421.

M. S. Hanner and C. Polanskey, Jet Propulsion Laboratory, Pasadena, CA 91109.

M. Horányi, Laboratory for Atmospheric and Space Physics, University of Colorado, Boulder, CO 80309.

B. A. Lindblad, Lund Observatory, 221, Lund, Sweden.

I. Mann, Max-Planck-Institut für Aeronomie, 37191 Katlenburg-Lindau, Germany.

J. A. M. McDonnell, Unit for Space Science and Astrophysics, University of Kent, Canterbury, CT2 7NR, England, United Kingdom.

G. E. Morfill, Max-Planck-Institut für Extraterrestrische Physik, 85740 Garching, Germany.

G. Schwehm, European Space Research and Technology Centre, 2200 AG Noordwijk, The Netherlands.

H. A. Zook, NASA Johnson Space Center, Houston, Texas 77058.

(Received August 8, 1997; revised December 3, 1997; accepted January 2, 1998.)